THE PRESSURE AND MG# DEPENDENCE OF ILMENITE AND ILMENITE-OLIVINE AGGREGATE RHEOLOGY: IMPLICATIONS FOR LUNAR CUMULATE MANTLE OVERTURN. L. Tokle[1], G. Hirth[1], P. Raterron[1,2], N. Dygert[3], Y. Liang[1], and C. W. Holyoke[4], [1]Department of Earth, Environmental and Planetary Sciences, Brown University (Leif_Tokle@brown.edu); [2]Unité Matériaux Et Transformations (UMET), ENSCL, CNRS, Université Lille; [3]Jackson School of Geosciences, University of Texas at Austin; [4]Department of Geosciences, University of Akron.

Introduction: Ilmenite has been inferred to be an important component of the lunar basalt source region [1,2]. According to magma ocean crystallization models, dense Fe-rich olivine, clinopyroxene, and ilmenite referred to as Ilmenite-bearing cumulates (IBC) overlie less dense mafic cumulates, producing an unstable density stratification [3,4]. It is hypothesized that lunar cumulate mantle overturn could result from this instability [2,4].

Prior to the recent study [5], the rheology of ilmenite was unknown and only a few studies have investigated the effects of Fe-content on olivine rheology [6,7]. The results from [5] show that for dislocation creep in both ilmenite and olivine, ilmenite is approximately 3.5-orders of magnitude less viscous than dry San Carlos (SC) olivine. [6] has shown for GBS in olivine that fayalite is also approximately 3.5-orders of magnitude less viscous than SC olivine. According to [5] and [6], ilmenite and fayalite are nearly isoviscous at similar experimental conditions. Ongoing work by Raterron et al. [8] show that at higher pressures (2.5-5 GPa) the variation in viscosity between fayalite and SC decreases to less than an order of magnitude at T =1100-1200°C.

Previous efforts to study cumulate mantle overturn applied various SC olivine rheologies [9,10], which likely predicted higher viscosities that are not representative of the IBC layer, or explored various effects on the viscosities of lunar mantle convection patterns [4,11-13]. These studies produced a wide range of possible scenarios that can be evaluated with the new experimental results. To more accurately constrain the thermochemical evolution of the lunar mantle, a better understanding of the rheological effects of relevant lunar compositions for the IBC and the underlying mafic cumulates are required.

Experiments: To study the rheology of ilmenite and olivine aggregates at lunar mantle conditions, deformation experiments were performed in the Deformation-DIA (D-DIA) apparatus at the 6BM-B beamline of the Advanced Proton Source (APS) at Argonne National Laboratory. Experiments were performed in axisymmetric compression at T = 800 and 1100°C, with confining pressures from 2.0 to 5.3 GPa and strain rates within 0.2 to 1.5 x 10^{-4} s^{-1}. Two samples were aligned, one on top of the other in the compression column of the D-DIA cubic cell, in between two alumina pistons. The sample powders and pistons were divided by Ni- and Re-disks and wrapped in Ni-foil to maintain the oxygen fugacity, f_{O2}, below the Ni/NiO buffer. Pressure and stress during each experiment were measured *in situ* from *d*-spacing variations for given (*hkl*) planes in different orientations with respect to the principal stress directions. The strain and strain rates for each sample were measured from the change in length observed *in situ* by time-resolved X-ray radiography [14].

All powders were either synthesized from oxides or for SC olivine powder, obtained by grinding a natural single crystal, then sieved to a grain size of 20-30μm. Two suites of powders were synthesized, an Mg-free suite ($FeTiO_3$ / Fe_2SiO_4) and a Mg-present suit ($Fe_{0.4}Mg_{0.6}TiO3$ / $Fe_{0.1}Mg_{0.9}SiO_4$), where ilmenite and olivine are in chemical equilibrium. Deformation experiments were conducted either with pure phases or with a mixture of two phases. For mixture experiments, ilmenite and olivine powders were mechanically mixed with different fractions of ilmenite ranging from 5 to 50 vol.%, in order to compare the relative viscosity of a mixed aggregate with that of the pure ilmenite aggregate. No water was added; samples were placed in an oven at ~120°C for 2 hours prior to loading into the D-DIA.

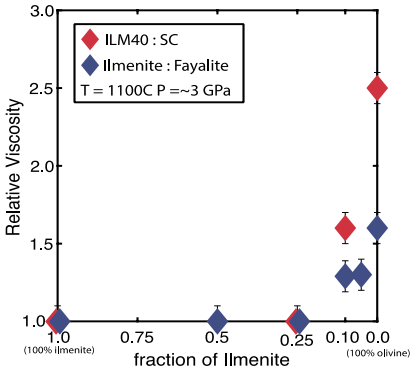

Figure 1. Relative viscosity of ilmenite and olivine + ilmenite samples vs. fraction of ilmenite in the mixed sample.

Results: For each D-DIA experiment, we assume that the two samples experience approximately the same pressure, temperature, and stress throughout the experiment. Therefore, the variation in strain rate also constrains the relative effective viscosity between the two samples. Figure 1 shows the relative effective viscosities for the mixture experiments for the Mg-free and Mg-present mixtures. The Mg-present samples have a larger relative viscosity for the endmember case;

however, both suites of mixture experiments produce an isoviscous aggregate when there is between 10% and 25% ilmenite by volume. The relative differences in viscosity at these conditions are small, at most only a factor of 2.5, in comparison to the three-orders of magnitude difference predicted by the flow laws for ilmenite and dry SC olivine [5]. These experiments likely, place a lower limit on the weakening effect of ilmenite because the total strain in the samples is low (ε~0.5).

We calculate an activation volume,V*, for ilmenite of $17.2\pm3.9 \times 10^{-6}$ and $9.0\pm5.1 \times 10^{-6}$ cm^3/mol for $FeTiO_3$ (Ilm100) and $Fe_{0.4}Mg_{0.6}TiO_3$ (Ilm40), respectively (inset of figure 2). Modifying the Ilmenite flow law for dislocation creep [5] using the newly calculated V* and correcting the data to P = 1 GPa and T = 1100°C, the data largely fall on the flow law or within its error for all experiments conducted between 2.0 and 5.3 GPa at T = 1100°C (Figure 2). Experiments conducted at 800°C all plot above the ilmenite flow law which we interpret to reflect power law break down (Figure 2).

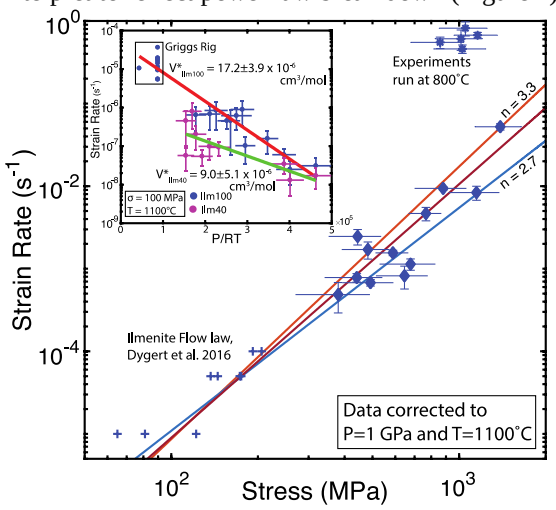

Figure 2. Strain rate vs. stress plot for all low-P ([5], crosses) and high-P (this study, diamonds) for Ilm100 data obtained at T=1100°C corrected to P=1GPa. Superimposed to the data is the flow law for dislocation creep in ilmenite [5] modified using the activation volume, V*, obtained for Ilm100 (inset). Also plotted are the Ilm100 data obtained here at T=800°C (stars). The inset shows strain rate vs. P/RT for Ilm100 and Ilm40, as corrected to a stress of 100 MPa and T=1100°C. The slope is the negative activation volume.

Figure 3 shows the ilmenite and dry SC olivine flow laws for dislocation creep at various pressures [5,15]. The D-DIA data for ilmenite shows good agreement between the data and the flow law at all experimental pressures. The mechanical data for SC olivine, however, are significantly weaker than the dry flow law. Mechanical data from similar experiments conducted by [14] on SC olivine at higher pressures (blue circles in Fig. 3), show good agreement with the mechanical data from this study (blue diamonds in Fig. 3). [14] determined that the SC olivine in their experiments were wet. We are currently conducting transmission FTIR analysis on olivine samples with preliminary analysis showing the presence of water.

Implications: The presence of ilmenite in the IBC layer will reduce the effective viscosity of this layer. The influence of ilmenite depends on the Mg# of the system and phase proportions. Our current results lead us to favor long wavelength overturn of the cumulate mantle [13]. Overturn of the IBC layer would place pyroxene-hosted heat producing elements at the core-mantle boundary which could help explain the presence of an ultralow viscosity zone around the core [16] and the potential for developing a seismically attenuating partially molten layer around the core [17,18]. The abundance of water in the lunar mantle is still debated and further work is needed to evaluate the effects water may have on the characteristics of cumulate mantle overturn.

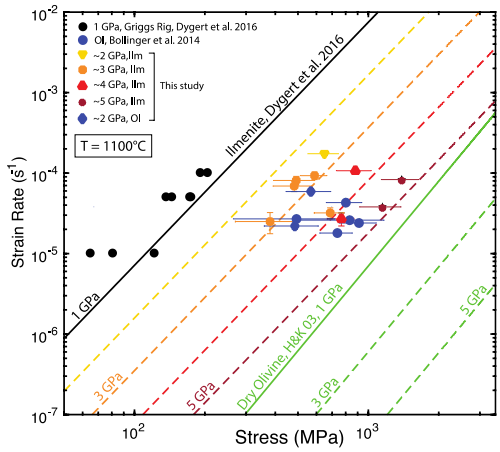

Figure 3. Plot of dislocation creep flow laws for ilmenite [5] and dry SC olivine [15]. V*=15cm^3/mol was use for the olivine flow law. Ilmenite data is color-coded to the ilmenite flow law with approximately the same confining pressure.

References: [1] Ringwood and Kesson (1976) LPS VII, 1697-1722. [2] Hubbard and Minear (1975) LPS, VI, 1057-1085. [3] Snyder et al. (1992) GCA 56, 3809-3823. [4] Hess and Parmentier (1995) EPSL, 134, 501-514. [5] Dygert et al. (2016) GRL, 43, 532-540. [6] Zhao et al. (2009) EPSL, 287, 229-240. [7] Tasaka et al. (2015) JGR, 120, 1-19. [8] Raterron et al. (2017) LPSC abstract. [9] Elkins-Tanton et al. (2002) EPSL 196, 239-249. [10] de Vries et al. (2009) EPSL 292, 139-147. [11] Zhong et al. (2000) EPSL 177, 131-140. [12] Zhang et al. (2013) JGR 118, 1789-1804. [13] Parmentier et al. (2002) EPSL 201, 473-480. [14] Bollinger et al. (2014) PEPI, 228, 211-219. [15] Hirth and Kohlstedt (2003) Geophys. Monograph 138, 83-105. [16] Harada et al. (2014) *Nat. Geosci.* 7, 569-572. [17] Nakamura et al. (1973) *Sci.* 181, 49-51. [18] Weber et al. (2011) *Sci.* 331, 309-312.